

BROADBAND CLOAKING FOR FLEXURAL WAVES

AHMAD ZAREEI & MOHAMMAD-REZA ALAM

Department of Mechanical Engineering, University of California, Berkeley

ABSTRACT. The governing equation for elastic waves in flexural plates is not form invariant, and hence designing a cloak for such waves faces a major challenge. Here, we present the design of a perfect broadband cloak for flexural waves through the use of a nonlinear transformation, and by matching term-by-term the original and transformed equations. For a readily achievable flexural cloak in a physical setting, we further present an approximate adoption of our perfect cloak under more restrictive physical constraints. Through direct simulation of the governing equations, we show that this cloak, as well, maintains a consistently high cloaking efficiency over a broad range of frequencies. The methodology developed here may be used for steering waves and designing cloaks in other physical systems with non form-invariant governing equations.

1. INTRODUCTION

The method of *Transformation Optics*, originally developed in optics community for passive cloaking (Pendry et al., 2006; Leonhardt, 2006), offers a novel method for controlling electromagnetic waves using the subtle idea of coordinate transformation. Based on this method, invisibility cloaks for electromagnetic waves were designed, fabricated and successfully tested (Schurig et al., 2006; Liu et al., 2009).

The most important necessary condition for applicability of the method of transformation optics is that the governing equations must be *form invariant* under coordinate transformation. Since physical systems admitting wave solutions share many common properties, it is well expected that the transformation optics method works in any wave system with form-invariant governing equation. This has been confirmed and cloaks have been designed and tested in a variety of other systems such as for acoustic waves (Cummer and Schurig, 2007; Chen and Chan, 2007; Huang et al., 2014), water waves (Chen et al., 2009; Berraquero et al., 2013; Zareei and Alam, 2015) and matter waves (Zhang et al., 2008).

Flexural waves, such as those propagating on a thin elastic plates, have a governing equation that is known to be not form-invariant (e.g. Milton et al., 2006). Therefore, the classical method of designing a cloak through transformation media method does not directly work in the context of flexural waves. One crude approximation is to adopt a form-invariant equation whose form is close to the governing equation of flexural waves and then use classical linear cloak design (Farhat et al., 2009; Stenger et al., 2012). While the resulting wave pattern about a to-be-cloaked cylinder may look like wave patterns of cloaking, a quantitative investigation of cloaking efficiency¹ (Norris and Vemula, 1995) reveals that such a cloak has a poor and in many cases even *negative* cloaking efficiency (i.e. an object with the cloak about it scatters even more energy than the object without one, see also fig. 3, 4). Alternatively, if it is assumed that both density and elasticity of the material can be independently tuned, then a condition is obtained under which the highest order term of the governing equation satisfies the cloaking requirement (Brun et al., 2014). This is theoretically an improvement, as the highest order term can be shown to play a more important role than the rest of the terms in the governing equation. Nevertheless, fabricating a material with a variable density *and* elasticity is a serious challenge (Stenger et al., 2012). Along the same line, more degrees of freedom such as several independent elastic parameters may be assumed to improve the theoretical performance (Colquitt et al., 2014), but this makes the realization of the cloak in physical space even farther from achievable.

Here we present the design of a perfect broadband cloak for flexural waves. For the cloak to be realizable in the physical domain, we put the constraint that the density ρ is constant and only the modulus of elasticity E can be changed across the cloak. We employ a nonlinear transformation and, by choosing proper material properties and

E-mail address: ahmad.zareei@gmail.com, reza.alam@berkeley.edu.

¹Cloaking efficiency is defined as the ratio of *reduction in the energy scattered to infinity in the presence of cloak to energy scattered to infinity in the absence of the cloak*. A perfect cloak has an efficiency of 100%.

pre-stressing, match term-by-term the coefficients in the original and transformed equations. We show rigorously that the transformed equation matches perfectly with the orthotropic and inhomogeneous plate's equation.

2. GOVERNING EQUATIONS

For an isotropic plate with thickness h and density ρ_0 , governing equation for out of the plane displacement $\eta(R, \Theta, t)$ in the z direction normal to the plate's surface reads (e.g. Timoshenko and Woinowsky-Krieger, 1940)

$$(2.1) \quad D_0 \Delta^2 \eta + \rho_0 h \eta_{tt} = 0,$$

where $D_0 = E_0 h^3 / 12(1 - \nu^2)$ is the flexural rigidity, E_0 is the Young Modules, ν is the Poisson ratio, and Δ is the horizontal Laplacian operator in (R, Θ) directions.

To cloak a circular region A_c (radius a) with a cloak of outer radius b co-centered with A_c , we need to map the region of $0 \leq R \leq b$ to the cloaking region $a \leq r \leq b$. We use the nonlinear transformation \mathcal{F} defined as

$$(2.2) \quad \mathcal{F} : \begin{cases} r = \sqrt{(1 - a^2/b^2)R^2 + a^2}, & 0 \leq R \leq b, \\ \theta = \Theta, \end{cases}$$

that has a special property of its Jacobian being a constant (Zareei and Alam, 2015). Using this transformation and further assuming a time-periodic motion of frequency ω , equation (2.1) is mapped to (using Lemma 2.1 in Norris, 2008)

$$(2.3) \quad D_0 \tilde{\nabla}^2 \tilde{\nabla}^2 \eta - \rho_0 h \omega^2 \eta = 0,$$

where

$$(2.4) \quad \tilde{\nabla}^2 = \left(1 - \frac{a^2}{b^2}\right) \left[\frac{1}{r} \frac{\partial}{\partial r} \left(\frac{r^2 - a^2}{r} \frac{\partial}{\partial r} \right) + \frac{1}{r^2 - a^2} \frac{\partial^2}{\partial \theta^2} \right].$$

Note that if $a = 0$, then $\tilde{\nabla}^2 \equiv \Delta$.

In a traditional cloak design for form-invariant governing equations (e.g. Pendry et al., 2006), material properties as functions of spatial variables are determined such that the transformed equation (2.3) with the new material properties becomes equivalent of the original equation (2.1). If we do the same here, the rigidity D becomes spatially variable in different directions, which means the required material for cloaking is *inhomogeneous* and *orthotropic*. The issue is, equation (2.1) with $D = D(r, \theta)$, is *not* the governing equation for an inhomogeneous and orthotropic plate. In fact, the governing equation for a general $D(r, \theta)$ is very much different in the look [equation (4.3) in the Appendix], and most importantly this equation is *not* form-invariant.

With this knowledge, we therefore look for material properties that result in the matching of the coefficients of the two equations (i.e. (2.3) and (4.3)). We find that if we choose the following material parameters

$$(2.5a) \quad D_r = \alpha^2 \mathcal{A}^2(r) D_0,$$

$$(2.5b) \quad D_\theta = \alpha^2 (1/\mathcal{A}(r))^2 D_0,$$

$$(2.5c) \quad D_{r\theta} = \alpha^2 D_0,$$

$$(2.5d) \quad \nu_\theta = \frac{1}{\alpha^2 \mathcal{A}^2(r)} [\mathcal{B}(r) - 4 \log \mathcal{A}(r)],$$

where $\mathcal{A}(r) = 1 - (a/r)^2$, $\alpha = 1 - (a/b)^2$ and $\mathcal{B}(r) = 3(r/a) \log[(r-a)/(r+a)] - 2a^2/(r^2 - a^2)$ then between equation (2.3) and (4.3) all terms that include 4th order derivatives (i.e. highest order appearing in these equation), all 3rd order, 2nd order and 1st order terms match perfectly except two extra terms in the transformed equation which are factors of $\partial^2 \eta / \partial r^2$ and $\partial \eta / \partial r$. Interestingly, these extra terms go to zero if the penetration depth is small (see Eq. (4.10) in the Appendix). Alternatively, these two extra terms can be handled with a material that is pre-stressed in the radial direction (i.e. $N_{\theta\theta} = N_{r\theta} = 0$) with a radial body force (i.e. $S_\theta = 0$) according to

$$(2.6a) \quad \frac{N_{rr}}{D_0} = \frac{1}{2a^2} \left[\left(\frac{a}{r}\right)^8 \mathcal{N}(r) + \frac{3}{2} \left(\frac{a}{r}\right) \log \left(\frac{r-a}{r+a}\right) \right],$$

$$(2.6b) \quad \frac{S_r}{D_0} = -\frac{3}{a^3} \left(\frac{a}{r}\right)^{11} \mathcal{S}(r)$$

with $\mathcal{S}(r) = [5 - 12(r/a)^2 + 8(r/a)^4] / [1 - (a/r)^2]^2$ and $\mathcal{N}(r) = [6 - 10(a/r)^2 - 2(r/a)^4 + 3(r/a)^6] / [1 - (a/r)^2]$.

The above cloak for flexural waves is a rigorously derived *perfect* (i.e. efficiency is theoretically unity) and *broad-band* cloak. We now move to the next level by designing an approximate adoption of this perfect cloak restricted by

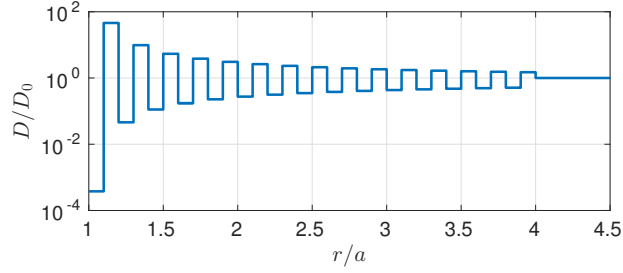


FIGURE 1. Profile of the rigidity as a function of r required to achieve a cloak for flexural waves. Each layer is made up of a homogeneous and isotropic material, but the averaged properties provides an inhomogeneous and orthotropic apparent rigidity according to (2.5). In the design presented here, the number of layers is 15, each layer is divided to two sub-layers, and $b/a = 4$.

more physical constraints that make achieving such a cloak even easier in an experimental setting. Specifically, the goal is to find an approximate adoption of our cloak that only requires *concentric layers of homogeneous material* (c.f. Stenger et al., 2012; Farhat et al., 2009). Using these concentric isotropic layers, we can only achieve a variable radial and azimuthal flexural rigidities.

Assuming only a variable radial and azimuthal rigidities in our cloak (i.e. equations (2.5a) and (2.5b)), only the highest derivatives (i.e. 4th order and 3rd order terms) match between equations (2.3) and (4.3). In order to test the effectiveness of our cloak which is based on the nonlinear transformation (2.2), in comparison with the one based on linear transformations (Stenger et al., 2012; Farhat et al., 2009), we use $N = 15$ layers of homogeneous but orthotropic materials, that is, D_r, D_θ are constant throughout each layer. To achieve the required orthotropic response, each layer is divided into two sub-layers of isotropic and homogeneous materials with different rigidities. These two sub-layers can be shown through homogenization that provide the required orthotropic properties (e.g. Cheng et al., 2008a). In implementing the cloak, since according to (2.5) the rigidities go unbounded at the inner boundary, a small offset is introduced such that the rigidity of the first layer (next to $r = a$) is calculated at this offset distance from the inner boundary. This offset can be shown to be equivalent of transforming a region of $\varepsilon \leq R \leq b$ to the cloaking region $a \leq r \leq b$ [see Eq. (5.1) and (5.2) in the Appendix]. In the numerical simulations that follow, we choose this offset to be 15% of thickness of a layer. The final profile of the rigidity of the isotropic and homogeneous layers for the case of $b/a = 4$ is shown in fig. 1.

3. NUMERICAL SIMULATION & RESULTS

In order to numerically solve the thin plate's equation with flexural rigidity as shown in fig. 1, we use the spectral method with Fourier expansion in the azimuthal direction and Bessel functions in the radial direction. Assuming time harmonicity of ω , the solution in each layer is therefore expressed as $\text{Re}[\eta(r, \theta) \exp(i\omega t)]$. We expand the spatial part $\eta(r, \theta)$ as

$$(3.1) \quad \eta(r, \theta) = \sum_{n=-\infty}^{\infty} \eta_n(r) \exp(in\theta),$$

where $\eta_n(r) = A_n J_n(k_i r) + B_n I_n(k_i r) + C_n Y_n(k_i r) + E_n K_n(k_i r)$ with $k_i^4 = \rho_0 h \omega^2 / D_i$ and D_i being the flexural rigidity of the layer. Here, $J_n(\cdot), Y_n(\cdot)$ and $I_n(\cdot), K_n(\cdot)$ are respectively Bessel and modified Bessel functions of the first and second kind. Also A_n, B_n, C_n and E_n are coefficients that are later found by satisfying the boundary conditions. These boundary conditions are continuity of displacement η , its radial derivative η_r , momentum M and shear force V at the boundaries [see Eq. (4.17) and (4.18) in the Appendix]. Note that spatial part of the incident planar wave can be written as $\eta^{inc} = a_0 \exp(ik_0 x) = a_0 \sum_{n=-\infty}^{\infty} i^n J_n(k_0 r) \exp(in\theta)$, where a_0 is the amplitude of the wave, $k_0^4 = \rho_0 h \omega^2 / D_0$ and D_0 is the constant flexural rigidity outside the cloak.

In order to quantitatively analyze the efficiency of the cloak, we calculate the scattering cross section which corresponds to the energy scattered to the infinity. The scattering displacement field is $\eta^{sc} = \eta - \eta^{inc}$, where η^{inc} is the incident plane wave. The scattered far field amplitude $f(\theta)$ is defined through (see e.g. Norris and Vemula, 1995)

$$(3.2) \quad \eta^{sc} = \frac{a_0}{\sqrt{2r}} e^{i(k_0 r - \pi/4)} f(\theta) + \mathcal{O}(1/\sqrt{r})$$

and the total scattering cross section is $\sigma^{sc} = 1/2\pi \oint |f(\theta)|^2 d\theta$.

We present here a side-by-side comparison of surface elevation η and scattered far field amplitude $f(\theta)$ for three cases: i. in the absence of cloak, ii. with the claimed linear cloak of (Farhat et al., 2009; Stenger et al., 2012), and iii. with our nonlinear cloak. We implement the linear cloak according to Eq. (4) of Farhat et al. (2009) for a cloak size of $b/a = 4$. We approximate the cloak $N = 15$ concentric layers that are homogeneous but anisotropic and then we use two isotropic and homogeneous sub-layers to approximate each of the 15 layer (see e.g. Farhat et al., 2009; Stenger et al., 2012; Cheng et al., 2008b). The resulted layers of isotropic and homogeneous materials approximates the anisotropic inhomogeneous cloak. We do the same for the nonlinear cloak but in this case according to equation 2.5. The result for a linear cloak design (Farhat et al., 2009; Stenger et al., 2012) and the nonlinear cloak for the range of the frequencies of $f = 200\text{Hz} - 500\text{Hz}$ alongside with the case when there is no cloak is shown in fig. 2 for comparison.

Looking at the displacement field in fig 2, both of the cloaks seems to be effective at lower frequencies. In fact, the linear cloak *looks* to be more effective than the nonlinear cloak in $f=200\text{Hz}$. More specifically, the nonlinear cloak appears to have less scattering downstream of the cylinder compared to the linear cloak and the linear cloak have less scattering upstream of the cylinder compared to the nonlinear case. By increasing the frequency, we observe that downstream scattering of the nonlinear cloak is much better in preserving the wave shape; while at the upstream of the cylinder the linear cloak has less scattering.

In order to quantitatively test the effectiveness of the cloaks, we present in fig. 3 the absolute value of the scattering amplitude $|f(\theta)|$ at different angles for both of the cloaks at different frequencies $f = 200\text{Hz} - 500\text{Hz}$. As is seen, in all of the frequencies, although in upstream of the cylinder the linear cloak is reducing the amount of energy scattered to infinity compared to the nonlinear case, far more energy is scattered in the downstream of the cylinder in the linear cloak, even larger than the case when there is no cloak. Therefore, in all cases the linear cloak scatters *more* energy to the downstream compared to when the cloak does not exist. Our nonlinear cloak consistently achieves a lower scattering in all angles with no exception.

In order to quantitatively see the net effect of the cloak in terms of the total energy scattered to the infinity, we also calculate and plot the total scattering cross section σ^{sc} (fig. 4). In the frequencies bellow 200Hz, although the linear cloak scatters more energy at certain angles (at the downstream side of the cylinder) compared to the case with no cloak [see fig 3], the total energy scattered to the infinity is smaller than the case with no cloak. At frequencies above 200Hz the linear cloak both scatters far more energy at the back of the cylinder and also in total. Note that, the total scattering cross section for the nonlinear cloak stays always smaller than the case without any cloak. This underlines the broadband effectiveness of our proposed nonlinear cloak.

In summary, we presented here the design of a perfect broadband cloak for flexural waves. Since the governing equations for flexural waves are not form-invariant, the traditional cloak design methodology through linear transformation optics scheme does not apply here. We therefore employed a nonlinear transformation and matched, term-by-term, the transformed equation with the true governing equation for an inhomogeneous and orthotropic plate equation. We showed rigorously that the resulting cloak is perfect. We also presented an adoption of our perfect cloak obtained under more restrictive physical constraints that make the design more amenable for experimental investigations. These constraints are that cloak can only include a finite number of concentric layers of homogeneous materials and that only modulus of elasticity can be variable from layer to layer. We presented this approximate cloak, and showed via direct simulation that this experimentally realizable cloak of such type has a consistent performance in all spatial directions, and also has a broad bandwidth of high efficiency.

The nonlinear cloak proposed in here is combination of layers of homogeneous and isotropic materials, which are amenable to physical fabrication and testing and real-life application (e.g. potentially in cloaking against earthquakes Br  l   et al., 2014; Colombi et al., 2015). The nonlinear transformation proposed here, may be applied for other types of the waves to soften the required material properties. For instance, in electromagnetism, with this nonlinear cloak, we can remove one degree of the freedom and keep permeability (permittivity) as a constant in cloaking for transverse magnetic (electric) waves.

4. APPENDIX

GOVERNING EQUATION

Assuming an orthotropic and inhomogeneous plate, under pure bending and in the absence of in-plane forces, we have (Liessa, 1969)

$$(4.1) \quad \frac{\partial^2 M_R}{\partial R^2} + \frac{2}{R} \frac{\partial M_R}{\partial R} + \frac{2}{R} \frac{\partial^2 M_{\Theta R}}{\partial R \partial \Theta} + \frac{2}{R^2} \frac{\partial M_{\Theta R}}{\partial \Theta} + \frac{1}{R^2} \frac{\partial^2 M_{\Theta}}{\partial \Theta^2} - \frac{1}{R} \frac{\partial M_{\Theta}}{\partial R} + \rho_0 h \omega^2 \eta = 0,$$

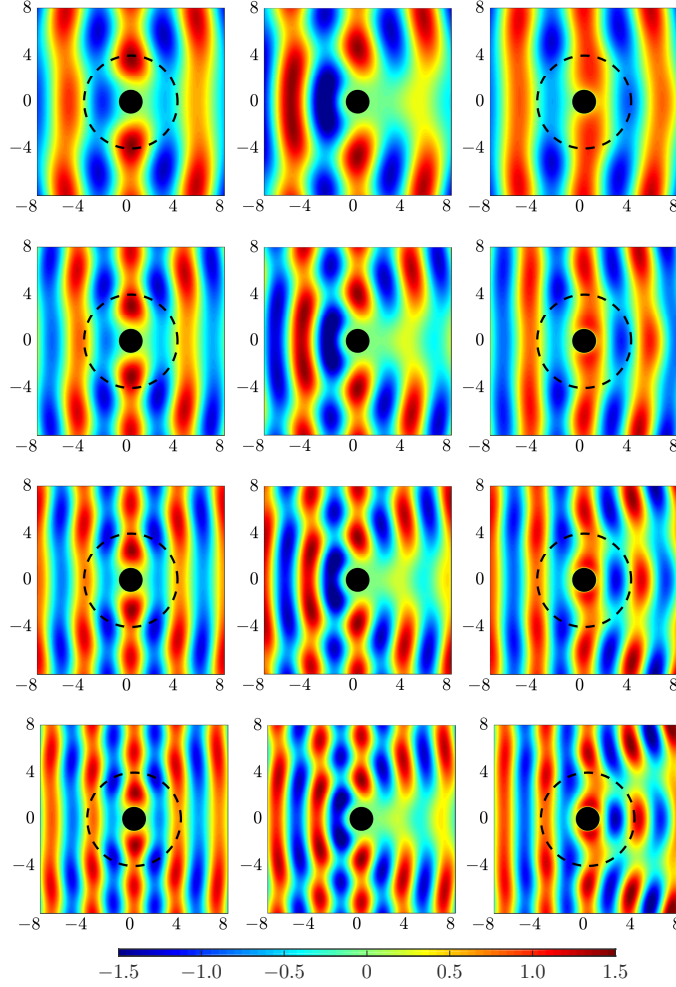


FIGURE 2. Nondimensionalized displacement field η/a_0 for a nonlinear cloak (left column), without any cloak (middle column), and linear cloak (right column). Each row corresponds to a different frequencies: 200Hz (first row), 300Hz (second row), 400Hz (third row) and 500Hz (the last row). Coordinates are nondimensionalized with radius of the inner cylinder a and the cloak size for both linear and nonlinear cloak is $b/a = 4$. The cloaks are approximated with $N = 15$ layers of homogeneous anisotropic materials with each layer composed of two sub-layers made up of different homogeneous and isotropic materials. For a direct comparison with Stenger et al. Stenger et al. (2012), Frequencies are obtained using the values of $h = 1mm$, $a = 1.5cm$, $\rho = 2000kg/m^3$ and $D_0 = 0.1037Nm^2$. A nonlinear cloak shows a consistent cloaking efficiency for different frequencies, while performance of the linear cloak drops significantly as the frequency increases. For a quantitative comparison of performance, see figures 3,4.

where M_R, M_Θ and $M_{R\Theta}$ are the bending moments, ρ_0 is the density of the plate, h is the thickness and ω is the frequency of the wave. Bending moments M_R, M_Θ and $M_{R\Theta}$ are found as

$$(4.2a) \quad M_R = -D_R \left[\frac{\partial^2 \eta}{\partial R^2} + \nu_\Theta \left(\frac{1}{R} \frac{\partial \eta}{\partial R} + \frac{1}{R^2} \frac{\partial^2 \eta}{\partial \Theta^2} \right) \right],$$

$$(4.2b) \quad M_\Theta = -D_\Theta \left(\frac{1}{R} \frac{\partial \eta}{\partial R} + \frac{1}{R^2} \frac{\partial^2 \eta}{\partial \Theta^2} + \nu_R \frac{\partial^2 \eta}{\partial R^2} \right),$$

$$(4.2c) \quad M_{R\Theta} = -2D_K \frac{\partial}{\partial R} \left(\frac{1}{R} \frac{\partial \eta}{\partial \Theta} \right),$$

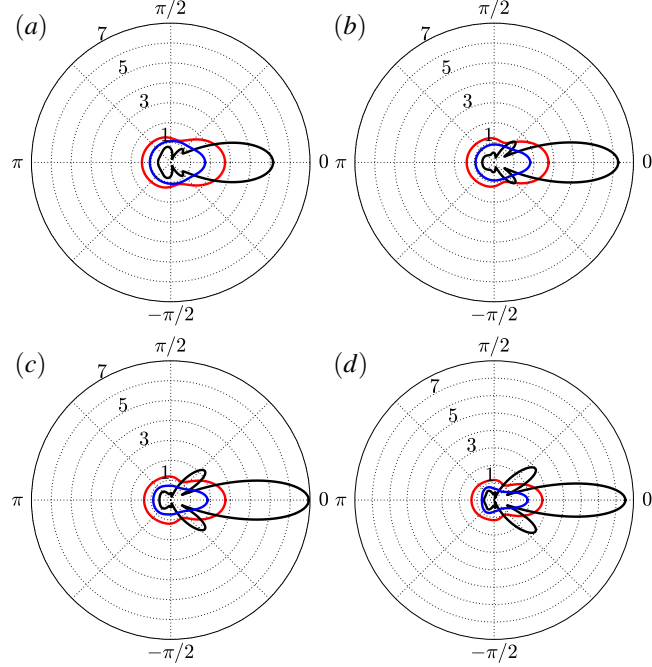


FIGURE 3. Polar plot of absolute value of scattering amplitude $|f(\theta)|$ for the linear cloak (—), without cloak (—), and with nonlinear cloak (—) for different frequencies of (a) 200Hz, (b) 300Hz, (c) 400Hz and (d) 500Hz.

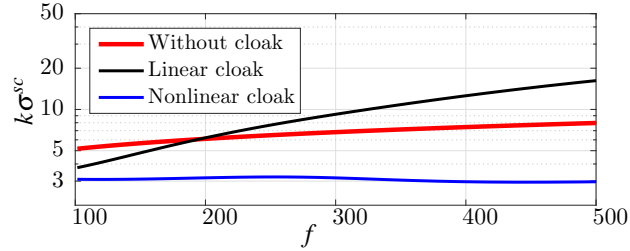


FIGURE 4. Nondimensionalized total scattering cross section with wavelength i.e. $k\sigma^{sc}$ for a range of frequencies for 3 different cases of without cloak, with a linear cloak and with a nonlinear cloak.

where $\eta(R, \Theta)$ is the out-of-plane displacement, D_R, D_Θ are the flexural rigidities in the R, Θ directions respectively, D_K is the shearing rigidity and ν_R, ν_Θ are the Poisson ratios in the radial and tangential directions. Note that the radial and tangential rigidities D_R, D_Θ satisfy the symmetry relation $D_R\nu_\Theta = D_\Theta\nu_R$. Using these relations and defining $D_{R\Theta} = 2D_K + D_R\nu_\Theta$, equation (4.1) simplifies to (Brun et al., 2014)

$$\begin{aligned}
 & D_R \frac{\partial^4 \eta}{\partial R^4} + \frac{D_\Theta}{R^4} \frac{\partial^4 \eta}{\partial \Theta^4} + \frac{2D_{R\Theta}}{R^2} \frac{\partial^4 \eta}{\partial R^2 \partial \Theta^2} + \left(\frac{2D_R}{R} + 2 \frac{\partial D_R}{\partial R} \right) \frac{\partial^3 \eta}{\partial R^3} \\
 & + \left(\frac{2}{R^2} \frac{\partial D_{R\Theta}}{\partial R} - \frac{2D_{R\Theta}}{R^3} \right) \frac{\partial^3 \eta}{\partial R \partial \Theta^2} + \left[\frac{1}{R^2} \frac{\partial}{\partial R} \left(R^2 \frac{\partial D_R}{\partial R} \right) + \frac{1}{R} \frac{\partial (D_R \nu_\Theta)}{\partial R} - \frac{D_\Theta}{R^2} \right] \frac{\partial^2 \eta}{\partial R^2} \\
 & + \left(\frac{2D_{R\Theta}}{R^4} - \frac{2}{R^3} \frac{\partial D_{R\Theta}}{\partial R} + \frac{2D_\Theta}{R^4} - \frac{1}{R^3} \frac{\partial D_\Theta}{\partial R} + \frac{1}{R^2} \frac{\partial^2 (D_R \nu_\Theta)}{\partial R^2} \right) \frac{\partial^2 \eta}{\partial \Theta^2} \\
 & + \left(\frac{D_\Theta}{R^3} - \frac{1}{R^2} \frac{\partial D_\Theta}{\partial R} + \frac{1}{R} \frac{\partial^2 (D_R \nu_\Theta)}{\partial R^2} \right) \frac{\partial \eta}{\partial R} - \rho_0 h \omega^2 \eta = 0.
 \end{aligned}
 \tag{4.3}$$

Assuming a constant rigidity $D_R = D_\Theta = D_{R\Theta} = D_0$, equation (4.3) simplifies to the famous biharmonic plate's equation as

$$(4.4) \quad D_0 \Delta^2 \eta - \rho_0 h \omega^2 \eta = 0.$$

Now as we aim to cloak a circular region A_c with radius a , with a cloak of outer radius b co-centered with A_c , we use the following transformation \mathcal{F} to map the area $0 \leq R \leq b$ to the cloaking region $a \leq r \leq b$ (Zareei and Alam, 2015)

$$(4.5) \quad \mathcal{F} : \begin{cases} r = f(R) = \sqrt{(1 - a^2/b^2)R^2 + a^2}, & 0 \leq R \leq b, \\ \theta = \Theta. \end{cases}$$

The Jacobi of the transformation \mathcal{F} in the polar coordinate is

$$(4.6) \quad \mathbf{F} = \sqrt{1 - a^2/b^2} \begin{pmatrix} \sqrt{r^2 - a^2}/r & 0 \\ 0 & r/\sqrt{r^2 - a^2} \end{pmatrix}_{(\mathbf{e}_r, \mathbf{e}_\theta)},$$

where $\{\mathbf{e}_r = \mathbf{E}_R, \mathbf{e}_\theta = \mathbf{E}_\Theta\}$. Transforming the governing equation (4.4), we obtain (see Lemma 2.1 in Norris, 2008)

$$(4.7) \quad \tilde{\nabla}^2 \tilde{\nabla}^2 \eta - \rho_0 h \omega^2 \eta = 0,$$

where

$$(4.8) \quad \tilde{\nabla}^2 = \left(1 - \frac{a^2}{b^2}\right) \left[\frac{1}{r} \frac{\partial}{\partial r} \left(\frac{r^2 - a^2}{r} \frac{\partial}{\partial r} \right) + \frac{1}{r^2 - a^2} \frac{\partial^2}{\partial \theta^2} \right]$$

Defining the following parameters

$$(4.9a) \quad D'_r = \alpha^2 \mathcal{A}^2(r) D_0,$$

$$(4.9b) \quad D'_\theta = \alpha^2 (1/\mathcal{A}(r))^2 D_0,$$

$$(4.9c) \quad D'_{r\theta} = \alpha^2 D_0,$$

$$(4.9d) \quad v'_\theta = \frac{1}{\alpha^2 \mathcal{A}^2(r)} [\mathcal{B}(r) - 4 \log \mathcal{A}(r)],$$

where $\alpha = 1 - a^2/b^2$ and $\mathcal{A}(r) = 1 - a^2/r^2$ and $\mathcal{B}(r) = 3(r/a) \log \left(\frac{r-a}{r+a} \right) - 2a^2/(r^2 - a^2)$. We can further expand and simplify equation (4.7) as

$$(4.10) \quad \begin{aligned} & D'_r \frac{\partial^4 \eta}{\partial r^4} + \frac{D'_\theta}{r^4} \frac{\partial^4 \eta}{\partial \theta^4} + \frac{2D'_{r\theta}}{r^2} \frac{\partial^4 \eta}{\partial r^2 \partial \theta^2} + \left(\frac{2D'_r}{r} + 2 \frac{\partial D'_r}{\partial r} \right) \frac{\partial^3 \eta}{\partial r^3} \\ & + \left(\frac{2}{r^2} \frac{\partial D'_{r\theta}}{\partial r} - \frac{2D'_{r\theta}}{r^3} \right) \frac{\partial^3 \eta}{\partial r \partial \theta^2} + \left[\frac{1}{r^2} \frac{\partial}{\partial r} \left(r^2 \frac{\partial D'_r}{\partial r} \right) + \frac{1}{r} \frac{\partial (D'_r v'_\theta)}{\partial r} - \frac{D'_\theta}{r^2} + \mathcal{C}(r) \right] \frac{\partial^2 \eta}{\partial r^2} \\ & + \left(\frac{2D'_{r\theta}}{R^4} - \frac{2}{r^3} \frac{\partial D'_{r\theta}}{\partial r} + \frac{2D'_\theta}{r^4} - \frac{1}{r^3} \frac{\partial D'_\theta}{\partial r} + \frac{1}{r^2} \frac{\partial^2 (D'_r v'_\theta)}{\partial r^2} \right) \frac{\partial^2 \eta}{\partial \theta^2} \\ & + \left(\frac{D'_\theta}{r^3} - \frac{1}{r^2} \frac{\partial D'_\theta}{\partial r} + \frac{1}{r} \frac{\partial^2 (D'_r v'_\theta)}{\partial r^2} + \mathcal{D}(r) \right) \frac{\partial \eta}{\partial r} - \rho_0 h \omega^2 \eta = 0. \end{aligned}$$

where

$$(4.11a) \quad \mathcal{C}(r) = \frac{1}{2a^2} \left(\frac{a}{r} \right)^8 \left[\frac{6 - 10(r/a)^2 - 2(r/a)^4 + 3(r/a)^6}{1 - (a/r)^2} + \frac{3}{2} \left(\frac{r}{a} \right)^7 \log \left(\frac{r-a}{r+a} \right) \right] D_0,$$

$$(4.11b) \quad \mathcal{D}(r) = \frac{3}{a^3} \left(\frac{a}{r} \right)^{11} \frac{5 - 12(r/a)^2 + 8(r/a)^4}{(1 - a^2/r^2)^2} D_0.$$

Now, we observe that the transformed equation i.e. equation (4.10), matches with the inhomogenous and orthotropic plate's equation i.e. equation (4.3), with the rigidities and the Poisson ratio as defined in (4.9). The only difference is in the second order term $\partial^2 \eta / \partial r^2$ and the first order term $\partial \eta / \partial r$ with the coefficients defined in (4.11). Note that these remaining terms goes to zero as long as $r \gg a$, i.e. the penetration depth of the wave into the cloak is small.

These extra terms in equation (4.10) can also be interpreted as an additional pre-stress force \mathbf{N} and body force \mathbf{S} as

$$(4.12) \quad N_{rr} = \mathcal{C}(r), \quad N_{\theta\theta} = N_{r\theta} = 0,$$

$$(4.13) \quad S_r = -\mathcal{D}(r), \quad S_\theta = 0.$$

Note that the pre-stress force \mathbf{N} and the body force \mathbf{S} satisfy the following constraint as

$$(4.14) \quad \nabla \cdot \mathbf{N} + \mathbf{S} = 0.$$

NUMERICAL SOLUTION

Our cloak is composed of concentric layers of homogeneous materials with a clamped boundary condition at the inner most layer. We have planer incident waves and we aim to find the response of the cloak to the incoming waves.

For each layer, we expand the solution in that layer using spectral methods as

$$(4.15) \quad \eta^{(i)}(r, \theta) = \text{Re} \left\{ e^{i\omega t} \sum_{n=-\infty}^{\infty} \left[A_n^{(i)} J_n(k_i r) + B_n^{(i)} I_n(k_i r) + C_n^{(i)} Y_n(k_i r) + E_n^{(i)} K_n(k_i r) \right] e^{in\theta} \right\}$$

where $k_i^4 = \rho h \omega^2 / D_i$ with D_i being the flexural rigidity of the layer. Here, $J_n(\cdot)$, $Y_n(\cdot)$ and $I_n(\cdot)$, $K_n(\cdot)$ are respectively Bessel and modified Bessel functions of the first and second kind and $A_n^{(i)}$, $B_n^{(i)}$, $C_n^{(i)}$, $E_n^{(i)}$ are constants that are later found satisfying the boundary conditions.

Note that outside of the cloak, since the solution should remain finite and satisfy the radiation condition, the solution can be written as

$$(4.16) \quad \eta^{\text{out}}(r, \theta) = \text{Re} \left\{ e^{i\omega t} \sum_{n=-\infty}^{\infty} \left[F_n H_n^{(1)}(k_0 r) + G_n K_n(k_0 r) + a_0 i^n J_n(k_0 r) \right] e^{in\theta} \right\}$$

where $H_n^{(1)}(\cdot)$ is the Hankel function of the first kind, $k_i^4 = \rho h \omega^2 / D_i$ and D_i being the flexural rigidity outside of the cloak. Note that $a_0 i^n J_n(k_0 r)$ represents the planner incident wave. Boundary conditions at the boundary of each layer is continuity of η , its radial derivative η_r and also continuity of momentum and shear force as

$$(4.17) \quad M_r = -D \left[\frac{\partial^2 \eta}{\partial r^2} + \nu \left(\frac{1}{r} \frac{\partial \eta}{\partial r} + \frac{1}{r^2} \frac{\partial^2 \eta}{\partial \theta^2} \right) \right]$$

$$(4.18) \quad V = Q_r + \frac{1}{r} \frac{\partial M_{r\theta}}{\partial \theta}$$

where

$$(4.19) \quad Q_r = -D \frac{\partial}{\partial r} \nabla^2 \eta$$

$$(4.20) \quad M_{r\theta} = -D(1 - \nu) \frac{\partial}{\partial r} \left(\frac{1}{r} \frac{\partial \eta}{\partial \theta} \right)$$

Using the above boundary conditions at each layer and also the clamped boundary condition $\eta = \eta_r = 0$ at the boundary of the inner most layer, we can solve for the unknowns.

5. DISCUSSION ON TRANSFORMATION

In this section we show that the offset ε introduced earlier, is equivalent to transforming the region $\varepsilon \leq R \leq b$ to the cloaking region $a \leq r \leq b$, where ε is a small nonzero number. A transformations with a constant Jacobian, mapping the area $\varepsilon \leq R \leq b$ to the cloaking area $a \leq r \leq b$ can be written as

$$(5.1) \quad \mathcal{F} : \begin{cases} r = f(R) = \sqrt{c_1 R^2 + c_2}, & \varepsilon \leq R \leq b, \\ \theta = \Theta, \end{cases}$$

where

$$(5.2) \quad c_1 = \frac{b^2 - a^2}{b^2 - \varepsilon^2}, \quad c_2 = a^2 - \varepsilon^2 \frac{b^2 - a^2}{b^2 - \varepsilon^2}.$$

Note that when $\varepsilon = 0$, transformation (5.1) reduces to the transformation \mathcal{F} in equation (4.5). Picking a value of $\varepsilon/a = 0.175$, we observe that the profile of rigidity becomes the exact same as figure 1.

REFERENCES

- Berraquero, C. P., Maurel, a., Petitjeans, P., and Pagneux, V. (2013). Experimental realization of a water-wave metamaterial shifter. *Physical Review E*, 88(5):051002.
- Brûlé, S., Javelaud, E. H., Enoch, S., and Guenneau, S. (2014). Experiments on Seismic Metamaterials: Molding Surface Waves. *Physical Review Letters*, 112(13):133901.
- Brun, M., Colquitt, D. J., Jones, I. S., Movchan, a. B., and Movchan, N. V. (2014). Transformation cloaking and radial approximations for flexural waves in elastic plates. *New Journal of Physics*, 093020.
- Chen, H. and Chan, C. T. (2007). Acoustic cloaking in three dimensions using acoustic metamaterials. *Applied Physics Letters*, 91(18):183518.
- Chen, H., Yang, J., Zi, J., and Chan, C. T. (2009). Transformation media for linear liquid surface waves. *EPL (Europhysics Letters)*, 85(2):24004.
- Cheng, Y., Yang, F., Xu, J. Y., and Liu, X. J. (2008a). A multilayer structured acoustic cloak with homogeneous isotropic materials. *Applied Physics Letters*, 92(15):0–3.
- Cheng, Y., Yang, F., Xu, J. Y., and Liu, X. J. (2008b). A multilayer structured acoustic cloak with homogeneous isotropic materials. *Applied Physics Letters*, 92(15):151913.
- Colombi, A., Guenneau, S., Roux, P., and Richard, C. (2015). Transformation seismology: composite soil lenses for steering surface elastic Rayleigh waves. *Nature Publishing Group*, 9(April):1–19.
- Colquitt, D. J., Brun, M., Gei, M., Movchan, A. B., Movchan, N. V., and Jones, I. S. (2014). Transformation elastodynamics and cloaking for flexural waves. *Journal of the Mechanics and Physics of Solids*, 72:131–143.
- Cummer, S. A. and Schurig, D. (2007). One path to acoustic cloaking. *New Journal of Physics*, 9(3):45–45.
- Farhat, M., Guenneau, S., and Enoch, S. (2009). Ultrabroadband Elastic Cloaking in Thin Plates. *Physical Review Letters*, 103(2):024301.
- Huang, X., Zhong, S., and Liu, X. (2014). Acoustic invisibility in turbulent fluids by optimised cloaking. *Journal of Fluid Mechanics*, 749:460–477.
- Leonhardt, U. (2006). Optical conformal mapping. *Science*, 312(5781):1777–80.
- Liessa, A. W. (1969). Vibration of Plates NASA SP-160. Technical report, NATIONAL AERONAUTICS AND SPACE ADMINISTRATION.
- Liu, R., Ji, C., Mock, J. J., Chin, J. Y., Cui, T. J., and Smith, D. R. (2009). Broadband ground-plane cloak. *Science (New York, N.Y.)*, 323(5912):366–369.
- Milton, G. W., Briane, M., and Willis, J. R. (2006). On cloaking for elasticity and physical equations with a transformation invariant form. *New Journal of Physics*, 8(10):248–248.
- Norris, A. N. (2008). Acoustic cloaking theory. *Proceedings of the Royal Society A*, 464(2097):2411–2434.
- Norris, A. N. and Vemula, C. (1995). Scattering of flexural waves on thin plates. *Journal of Sound and Vibration*, 181:115–125.
- Pendry, J. B., Schurig, D., and Smith, D. R. (2006). Controlling electromagnetic fields. *Science*, 312(5781):1780–2.
- Schurig, D., Mock, J. J., Justice, B. J., Cummer, S. A., Pendry, J. B., Starr, A. F., and Smith, D. R. (2006). Metamaterial electromagnetic cloak at microwave frequencies. *Science (New York, N.Y.)*, 314(5801):977–80.
- Stenger, N., Wilhelm, M., and Wegener, M. (2012). Experiments on Elastic Cloaking in Thin Plates. *Physical Review Letters*, 108(1):014301.
- Timoshenko, S. and Woinowsky-Krieger, S. (1940). *Theory of Plates and Shells*. McGraw-Hill, New York, second edition.
- Zareei, A. and Alam, M.-R. (2015). Cloaking in shallow-water waves via nonlinear medium transformation. *Journal of Fluid Mechanics*, 778:273–287.
- Zhang, S., Genov, D. A., Sun, C., and Zhang, X. (2008). Cloaking of Matter Waves. *Physical Review Letters*, 100(12):123002.